BIOCHEMISTRY
including biophysical chemistry & molecular biology

Article

pubs.acs.org/biochemistry

# Effects of Calcium Binding and the Hypertrophic Cardiomyopathy A8V Mutation on the Dynamic Equilibrium between Closed and Open Conformations of the Regulatory N-Domain of Isolated Cardiac Troponin C

Nicole M. Cordina,[†] Chu K. Liew,[‡,∥] David A. Gell,[‡,⊥] Piotr G. Fajer,[§] Joel P. Mackay,[‡] and Louise J. Brown*[,†]

[†]Department of Chemistry and Biomolecular Sciences, Macquarie University, Sydney, NSW 2109, Australia

[‡]School of Molecular Bioscience, University of Sydney, Sydney, NSW 2006, Australia

[§]Institute of Molecular Biophysics, Florida State University, Tallahassee, Florida 32306-4380, United States

Supporting Information

**ABSTRACT:** Troponin C (TnC) is the calcium-binding subunit of the troponin complex responsible for initiating striated muscle contraction in response to calcium influx. In the skeletal TnC isoform, calcium binding induces a structural change in the regulatory N-domain of TnC that involves a transition from a closed to open structural state and accompanying exposure of a large hydrophobic patch for troponin I (TnI) to subsequently bind. However, little is understood about how calcium primes the N-domain of the cardiac isoform (cTnC) for interaction with the TnI subunit as the open conformation of the regulatory domain of cTnC has been observed only in the presence of bound TnI. Here we use paramagnetic relaxation enhancement (PRE) to characterize the closed to open transition of isolated cTnC in solution, a process that cannot be observed by traditional nuclear magnetic resonance methods. Our PRE data from four spin-labeled monocysteine constructs of isolated cTnC reveal that calcium binding triggers movement of the N-domain helices toward an open state. Fitting of the PRE data to a closed to open transition model reveals the presence of a small population of cTnC molecules in the absence of calcium that possess an open conformation, the level of which increases substantially upon $Ca^{2+}$ binding. These data support a model in which calcium binding creates a dynamic equilibrium between the closed and open structural states to prime cTnC for interaction with its target peptide. We also used PRE data to assess the structural effects of a familial hypertrophic cardiomyopathy point mutation located within the N-domain of cTnC (A8V). The PRE data show that the $Ca^{2+}$ switch mechanism is perturbed by the A8V mutation, resulting in a more open N-domain conformation in both the apo and holo states.

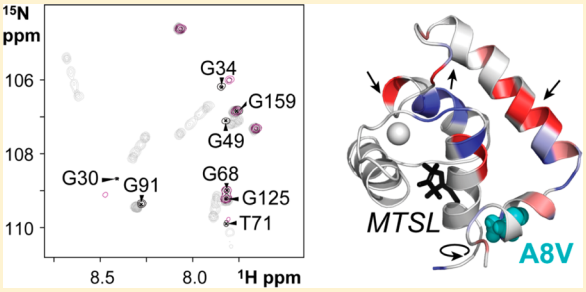


The control of the interaction between the actin and myosin filaments in both cardiac and skeletal muscle is a complex process, modulated by the $Ca^{2+}$ sensor troponin (Tn) protein complex. Tn is comprised of three subunits (TnC, TnI, and TnT) and is anchored to the thin filament at precise locations adjacent to the myosin interaction site via its troponin T (TnT) subunit. Striated muscle contraction is initiated by binding of $Ca^{2+}$ to the troponin C (TnC) subunit of the Tn complex. This event then induces conformational changes within TnC that relieve the inhibitory influence of the troponin I (TnI) subunit, thereby promoting formation of the actomyosin cross-bridge.[1]

The TnC subunit consists of two globular domains, the "structural" C-domain (C-TnC) and the "regulatory" N-domain (N-TnC), connected by a 10-residue flexible linker (Figure 1). Each of the TnC domains comprises two EF-hand metal binding motifs. The C-TnC contains two functional metal binding sites (sites III and IV) that are capable of binding $Ca^{2+}$ or $Mg^{2+}$ under all physiological conditions. In contrast, the two metal binding motifs in the N-TnC (sites I and II) are $Ca^{2+}$ specific and of lower affinity than the C-domain sites. It is the binding of $Ca^{2+}$ to the N-TnC that initiates the structural changes within TnC that allow for the switch region of TnI ($TnI_{switch}$, cardiac residues 150−165) to bind to the regulatory N-domain of TnC. The procurement of $TnI_{switch}$ by N-TnC subsequently releases the interaction of the inhibitory region of TnI (cardiac residues 137−148) from actin, relieving the actomyosin inhibition and allowing muscle contraction to occur.[1−4]

Both the N- and C-domains of the skeletal (skTnC) and cardiac (cTnC) isoforms of TnC have been extensively studied by nuclear magnetic resonance (NMR).[5−12] Both isoforms of

**Received:** January 6, 2013
**Revised:** February 14, 2013
**Published:** February 20, 2013

 © 2013 American Chemical Society  dx.doi.org/10.1021/bi4000172 | *Biochemistry* 2013, 52, 1950−1962

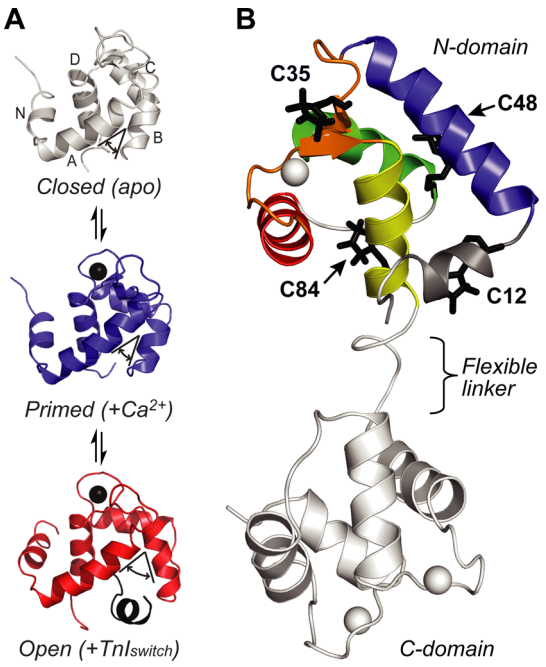


**Figure 1.** (A) Comparison of NMR structures for the regulatory N-domain of cardiac TnC in various physiological states: $Ca^{2+}$-free apo closed state (gray, PDB entry 1SPY[12]), site II-bound $Ca^{2+}$ holo primed state (blue, PDB entry 1AP4[12]), and $TnI_{switch}$ with $Ca^{2+}$ bound open state (red, PDB entry 1MXL[5]). $Ca^{2+}$ and TnI switch binding result in an increase in the A–B interhelical angle (~40°) and extension of helix B at the N-terminus. (B) Positions of the cysteine mutants created in this study. Helices N and A–D of the N-domain are colored gray, blue, green, red, and yellow, respectively. While there are two $Ca^{2+}$-binding loops in the N-domain (sites I and II, orange), only site II is capable of binding $Ca^{2+}$ in the cardiac isoform (gray sphere). Four monocysteine constructs (C12, C35, C48, and C84) were spin-labeled with MTSL (black) in intact cTnC.[9]

TnC show a similar spatial arrangement of their five N-domain $\alpha$-helices (N and A–D) in the metal-free state but a differing structural response upon $Ca^{2+}$ binding. In skeletal muscle, the binding of $Ca^{2+}$ to the two N-domain EF-hand metal sites (I and II) causes the N-domain to undergo a conformational change from a "closed" (apo) to an "open" (holo) conformation.[13] This $Ca^{2+}$-induced transition occurs because of the disruption of the small $\beta$-sheet that couples the two N-domain $Ca^{2+}$-binding loops and the extension of helices A–C. The opening of the domain then results from the large movement of helices B and C away from helices N, A, and B, through a 70° angle that subsequently exposes a large hydrophobic patch within the N-domain. Muscle contraction can then occur following the binding of $TnI_{switch}$ to the N-domain hydrophobic patch.[14]

In the cardiac isoform (cTnC), metal site I in the regulatory domain is incapable of binding $Ca^{2+}$, leaving only a single N-domain functional $Ca^{2+}$-binding site controlling muscle contraction. Further, NMR analysis of the N-domain of cTnC upon $Ca^{2+}$ binding indicated that no significant opening of the N-domain lobe takes place, in contrast to observations made on the skeletal isoform.[9] Instead, binding of $Ca^{2+}$ to site II of cTnC has been described to "prime" the N-domain for opening with only small structural changes reported. The changes include the partial disruption of the $\beta$-strand coupling metal sites I and II, the extension of the B-helix, and a small change in the A–B interhelical angle of only ~10°.[6] A "true" open conformation of the $Ca^{2+}$-bound form is, however, observed in the presence of the $TnI_{switch}$ region. The interaction of $TnI_{switch}$ with the N-domain of cTnC appears to be important in further disrupting the $\beta$-sheet, which thus allows the extension of helices A and C and the larger movement of the helices A and B toward the open state.[6] Thus, despite the lack of a significant conformational change upon $Ca^{2+}$ binding for cTnC in isolation, an open state is still ultimately taken up upon the hydrophobic interaction of the N-domain with the $TnI_{switch}$ region.[5]

Taken together, these data identify three physiologically relevant states of the N-domain of TnC for the cardiac isoform: an apo closed state, a $Ca^{2+}$-loaded "primed" state or "activated" closed structural state, and an open conformation in the presence of the $TnI_{switch}$ peptide (Figure 1A). However, while the existence of these three states is generally well accepted, the simple transition among these states under various conditions is not as easily described as the dynamic nature of cTnC introduces an additional level of complexity to this simplistic model.[11] In the presence of $Ca^{2+}$, NMR line broadening effects, indicative of conformational exchange, have been noted in cTnC for residues that correspond to the "hinges" involved in the domain opening transition.[8] It is therefore possible that cTnC does sample an open conformation upon $Ca^{2+}$ binding and that the interaction with $TnI_{switch}$ is an example of conformational selection rather than an induced fit mechanism.[8,15,16] What is unclear is how populated the open state is for cTnC, if it is indeed present, and how the nature of the closed to open equilibrium is modified by $Ca^{2+}$ binding.

The idea that N-cTnC undergoes dynamic exchange between closed and open states is also consistent with both nanosecond to microsecond motions detected by FRET[17] and RDC measurements,[16] but the existence of the open state in isolated N-cTnC is not corroborated by mutually exclusive NOEs corresponding to each conformational state.[8,9] However, the absence of such effects does not rule out the existence of conformational isomerism, considering that in the open conformation, very few interhelical contacts within the hinge region are below the 5 Å NOE upper limit.[18] Thus, to detect the open conformation, longer distance measurements are required. Here we describe the incorporation of paramagnetic nitroxide spin-labels into the N-domain of cardiac TnC and the measurement of paramagnetic relaxation enhancement (PRE)-derived distances in the range of 10–25 Å (Figure 1B). These measurements revealed the presence of a population of cTnC molecules possessing an open conformation that increases upon $Ca^{2+}$ binding. We have also characterized the structural consequences of a familial hypertrophic cardiomyopathy (FHC) mutation located within the N-domain of cTnC (TnC A8V).[19] Our results suggest that this mutation leads to a more open conformation in the absence and presence of $Ca^{2+}$.

## EXPERIMENTAL PROCEDURES

**Preparation of cTnC Constructs.** Rat cardiac TnC (cTnC) was expressed in the pET-3d expression vector (Novagen) as previously described.[20] As cTnC contains two native cysteine residues, the site specific spin labeling of TnC first required mutation of the two native cysteine residues to serine (C35S and C84S) to create a Cys-less cTnC construct (herein termed TnC*). We, and others, have shown that the conformation of TnC* does not differ significantly from that of the wild-type protein.[21−23]


dx.doi.org/10.1021/bi4000172 | Biochemistry 2013, 52, 1950−1962

To examine the conformation of the N-domain by PRE-NMR, two constructs from a recent study (C35 and C84) with a single cysteine located at position 35 or 84 were utilized.[23] Two additional monocysteine cTnC constructs (L12C and L48C), termed C12 and C48, respectively, were also generated, both conservative mutations. The FHC A8V mutation was introduced onto the C84 construct (TnC C35S A8V). All mutagenesis was performed using a QuikChange II site-directed mutagenesis kit (Stratagene), and mutations were verified by DNA sequencing before transformation into *Escherichia coli* BL21(DE3) cells for expression.

The cTnC constructs were expressed at 37 °C in M9 minimal medium containing 2.5 g/L glucose and 1 g/L $^{15}NH_4Cl$.[24] Expression was induced with 1 mM isopropyl $\beta$-D-1-thiogalactopyranoside (IPTG) once cells reached an optical density ($OD_{600}$) of 0.8. Cells were lysed (three passes at 15000 psi, EmulsiFlex-C3, Avestin), and insoluble cellular debris was removed by centrifugation before dialysis of the cell lysate against buffer A [0.2 M NaCl, 1 mM DTT, 5 mM $CaCl_2$, and 50 mM Tris-HCl (pH 7.5)]. cTnC was eluted from a 1.5 cm × 15 cm Phenyl Sepharose 6 Fast Flow column (GE Healthcare) by the addition of 10 mM EDTA. cTnC fractions were pooled and dialyzed against 0.35 M KCl, 1 mM DTT, 0.2 mM $CaCl_2$, 1 mM EDTA, and 50 mM Tris-HCl (pH 7.5) for loading onto a 2.5 cm × 7.5 cm DEAE-Sephadex A25 column (Sigma-Aldrich). Elution of cTnC was achieved with a linear KCl gradient from 0.35 to 0.60 M. Pure TnC fractions were identified using sodium dodecyl sulfate−polyacrylamide gel electrophoresis (SDS−PAGE) and concentrated to 5 mg/mL using an Amicon Ultra-15 centrifugal filtration device and protein concentrations determined using a BCA assay kit (Pierce).

**Spin Labeling of cTnC Constructs and Electron Paramagnetic Resonance (EPR) Spectroscopy.** For site specific labeling, the MTSL (1-oxyl-2,2,5,5-tetramethylpyrroline-3-methyl-16-methanethiosulfonate) (Toronto Research Chemicals) paramagnetic nitroxide moiety was covalently attached to the protein at the sulfhydryl group of the cysteine residue in each monocysteine cTnC construct. Briefly, cTnC was dialyzed against labeling buffer [100 mM KCl and 20 mM $KPO_4$ (pH 8)], and all cysteine sulfhydryl groups were reduced by incubation with 20 mM DTT for 2 h at room temperature. DTT was effectively removed using a 5 mL HiTrap desalting column (GE Healthcare) before incubation of cTnC overnight with a 10-fold molar excess of MTSL at room temperature. Excess MTSL was removed by exhaustive dialysis against the required NMR buffer.

The spin labeling efficiency of each spin-labeled cTnC sample was determined using a Bruker EMX X-band (9.5 GHz) EPR spectrometer with a standard rectangular TE cavity. First-derivative EPR absorption spectra were recorded at room temperature with a microwave power of 5.0 mW, a modulation amplitude of 1.0 G, and a sweep width of 140 G. EPR spectra were analyzed with a LabView package (National Instruments) of EPR spectral analysis programs. Spin labeling yields for each sample were determined from double integration of the EPR spectrum and interpolation with a calibration curve constructed from MTSL standards. In all cases, complete modification of each single cysteine construct was achieved (>95%).

**cTnC Sample Preparation for NMR Spectroscopy with or without $Ca^{2+}$.** MTSL-labeled TnC was dialyzed against 0.2 M EDTA for 2 h at 4 °C to chelate all $Ca^{2+}$ and $Mg^{2+}$ ions[25] and then exhaustively dialyzed into NMR buffer [50 mM KCl and 20 mM potassium phosphate (pH 6.7)], which had been pretreated with Chelex 100 resin (Bio-Rad), following the manufacturer's instructions. All glassware and plasticware were acid washed with 10% hydrochloric acid and rinsed thoroughly with decalcified Milli-Q $dH_2O$. NMR samples with $Ca^{2+}$ were supplemented with 1 mM $CaCl_2$ and samples without $Ca^{2+}$ with 3 mM $MgCl_2$. NMR samples were also checked for homogeneity by size exclusion chromatography on an analytical Superdex 75 10/300 column (GE Lifesciences) and non-reducing SDS−PAGE.[22] Aggregation was not observed in any instance. All NMR samples (500 $\mu$L) were prepared at concentrations ranging from 130 to 230 $\mu$M to prevent intermolecular PRE effects.[26] Immediately prior to the acquisition of NMR spectra, 10% $D_2O$ and 0.02 mM 2,2-dimethyl-2-silapentane-5-sulfonate (DSS) were added to each sample.

**NMR Spectroscopy.** NMR data were collected on a Bruker Avance 600 MHz spectrometer equipped with a cryoprobe. All experiments were performed at 30 °C. Spectra were processed using Topspin version 1.3 (Bruker Inc.), and spectral analysis was performed with Sparky.[27] After $^{15}N$ HSQC spectra of the paramagnetic state for samples with and without $Ca^{2+}$ had been acquired, the nitroxyl radical of MTSL was reduced to its hydroxylamine equivalent via the addition of a 5-fold molar excess of ascorbic acid (from a 0.5 M stock) directly to the NMR sample, incubated in the spectrometer at 30 °C for 1 h. The $^{15}N$ HSQC spectra were collected for the diamagnetic sample under both $Ca^{2+}$ conditions. The small volume of ascorbic acid (<0.5%) did not cause any detectable dilution effects, allowing direct comparison of peak intensities between paramagnetic and diamagnetic spectra used in the calculation of the relaxation enhancement. $^{15}N$ HSQC spectra were also acquired for each unlabeled single-cysteine TnC mutant to ensure the introduction of a mutant cysteine did not perturb the structure of the protein.

**Calcium Titration.** To allow assignment of spin-labeled samples in the state without $Ca^{2+}$, a calcium titration experiment was performed with apo cTnC* (230 $\mu$M). A $^{15}N$ HSQC spectrum was acquired of the apo sample, and then 12.5 mM $CaCl_2$ was added to directly to the NMR sample in a series of small aliquots (0.5−2.5 $\mu$L). $^{15}N$ HSQC spectra were acquired at 0.1, 0.2, 0.3, 0.4, 0.5, 0.7, 0.8, and 1.0 mM $CaCl_2$.

**PRE Data Analysis and Distance Determinations.** For each amide peak assigned in the $^{15}N$ HSQC spectra of the TnC constructs, the PRE caused by the MTSL spin-label ($\Gamma_2$) was calculated from peak heights in the paramagnetic state ($I_{para}$), as well as in the diamagnetic state after reduction of the spin-label ($I_{dia}$), using eq 1. The intrinsic transverse relaxation rate ($R_2$) was estimated from the $^1H$ peak width at half-height ($R_2 = \pi\Delta\nu_{1/2}$). All spectra were recorded with the single evolution time point ($t$) of 10 ms.[28,29]

$$\frac{I_{para}}{I_{dia}} = \frac{R_2 \exp(-\Gamma_2 t)}{R_2 + \Gamma_2} \quad (1)$$

The calculated PRE rates ($\Gamma_2$) were converted to distances ($r$) using a modified form of the Solomon−Bloembergen equation:[28−30]

$$\Gamma_2 = \frac{K}{r^6}\left(4\tau_c + \frac{3\tau_c}{1 + \omega_H{}^2\tau_c{}^2}\right) \quad (2)$$


dx.doi.org/10.1021/bi4000172 | *Biochemistry* 2013, 52, 1950−1962

where $\omega_H$ is the Larmor frequency of the proton, $K$ is a constant ($1.23 \times 10^{-32}$ cm$^6$ s$^{-2}$) that describes the spin properties of the nitroxide spin-label,[29] and $\tau_c$ is the correlation time of the electron−proton interaction [$\tau_c = (\tau_r^{-1} + \tau_s^{-1})^{-1}$]. Because of the slow electronic relaxation time of the nitroxide spin-label ($\tau_s$) compared to the protein rotational correlation time ($\tau_r$), the value of $\tau_c$ is effectively equal to $\tau_r$,[31] which was taken to be 5 ns, the correlation time reported for the regulatory domain of cardiac TnC at 30 °C.[11,32]

The $Q$ factor statistic was used to compare the N-domain (intradomain) PRE-measured distances ($r^{meas}$) to PDB ensembles of the regulatory N-domain of TnC in the apo state (PDB entry 1SPY[12]), in the $Ca^{2+}$-loaded state (PDB entry 1AP4[12]), and in the presence of both $Ca^{2+}$ and the TnI switch peptide (PDB entry 1MXL[5]). The position of the spin-label was modeled as previously described for each conformer within the PDB ensembles.[23] The PDB coordinates were then used to calculate the distance between the amide $H_N$ atom of each residue $i$ and the spin-label (calculated distances, $r^{calc}$). $Q$ factors ($Q$) were calculated to examine the agreement between the PDB-calculated distances ($r^{calc}$) and the PRE-measured distances ($r^{meas}$) using the following $Q$ factor statistic:[33]

$$Q = \sqrt{\frac{\sum_i (r_i^{meas} - r_i^{calc})^2}{\sum_i (r_i^{meas})^2}} \quad (3)$$

## RESULTS

**Calcium Titration of cTnC.** The goal of this study was to perform PRE measurements within the regulatory N-domain of TnC to reveal whether conformational changes take place upon $Ca^{2+}$ binding. We have previously made backbone assignments for cTnC in the $Ca^{2+}$-loaded state.[23] To assign the $^{15}N$ HSQC spectra of the state without $Ca^{2+}$, we titrated $Ca^{2+}$ into apo cTnC*. The exchange between $Ca^{2+}$-bound and -free forms of the N-domain was fast on the chemical shift time scale, allowing us to make assignments by simply tracking chemical shift changes during the course of the titration.

The majority of peaks in the apo cTnC* HSQC spectrum are well-dispersed (Figure S1a of the Supporting Information). However, there are ∼30 broadened and poorly dispersed peaks with HN chemical shifts of 7.5−8.2 ppm. Upon the first additions of $CaCl_2$ (0.1 mM $Ca^{2+}$ to a 0.15 mM cTnC* sample), the intensity of the broadened peaks decreased, while intensities of peaks corresponding to metal binding sites III and IV in the $Ca^{2+}$-saturated C-domain state increased (Figure S1 of the Supporting Information). This behavior suggests that the exchange between the $Ca^{2+}$-bound and $Ca^{2+}$-free states of C-domain sites III and IV occurs on a slow time scale and that these regions may be partially disordered in the absence of bound $Ca^{2+}$. The coupled peak intensity changes continued until a concentration of 2 molar equiv of $CaCl_2$ had been added (0.3 mM $Ca^{2+}$), indicating full occupancy of the C-domain metal sites. At this point during the titration, no further changes in N-domain resonances were observed. Our results from the titration of apo cTnC with $Ca^{2+}$ are consistent with the significantly higher $Ca^{2+}$ affinity of the two C-domain metal sites ($K_{Ca} = 1 \times 10^7$ M$^{-1}$) compared to that of the single N-domain site ($K_{Ca} = 2 \times 10^5$ M$^{-1}$).[34]

Following saturation of the C-domain sites with 2 molar equiv of $CaCl_2$, the addition of further $Ca^{2+}$ gave rise to chemical shift changes for N-domain resonances, corresponding to binding of $Ca^{2+}$ to site II (Figure 2). Mapping of the

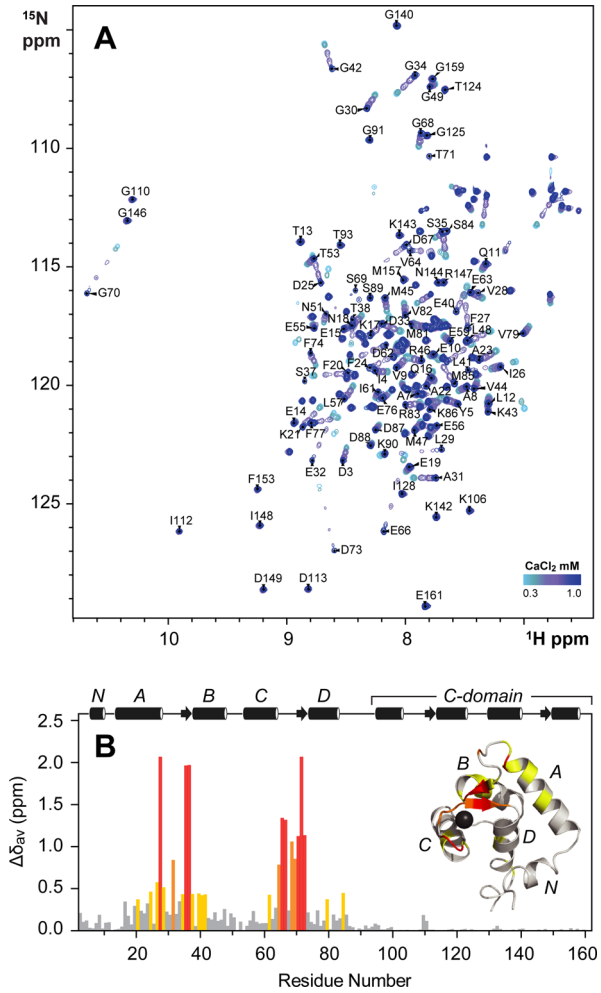


**Figure 2.** (A) Overlay of $^{15}N$ HSQC NMR spectra acquired during titration of $Ca^{2+}$ into the N-domain of TnC* (cTnC at a concentration of 0.15 mM). Residue assignments are shown for the saturated titration end point with $Ca^{2+}$.[23] (B) Combined $^1H$ and $^{15}N$ chemical shift differences ($\Delta\delta_{av}$) between the states of N-TnC* with $Ca^{2+}$ (holo) and without $Ca^{2+}$ (apo) [$\Delta\delta_{av} = (\Delta\delta_{HN}^2 + 0.17\Delta\delta_N^2)^{1/2}$, where $\Delta\delta_{HN}$ and $\Delta\delta_N$ are the chemical shift changes (in parts per million) for amide protons and nitrogens, respectively].[53] Significant chemical shift differences ($\Delta\delta_{av} > 1\sigma$, $2\sigma$, and $3\sigma$) are highlighted as yellow, orange, and red bars and are also mapped onto the N-domain of cTnC (PDB entry 1AJ4[9]).

chemical shift changes for each amide ($\delta_{av}$) caused by $Ca^{2+}$ binding to site II showed that the majority of significant shifts were observed for residues located at the active N-domain $Ca^{2+}$ site (site II). The largest shift changes were seen for E66, D67, T71, V72, and E73 of site II. Similar large shifts were also observed for several residues located in the defunct $Ca^{2+}$ site I (residues V28, I36, and S37) that can be attributed to the $\beta$-sheet coupling between the two N-domain metal sites.[6] Additionally, the chemical shift changes observed in helices A and B could result from the lengthening of these helices and consequent alterations to the interhelical angles, as previously observed to occur upon $Ca^{2+}$ binding.[6,12] Our findings here are consistent with previously reported $Ca^{2+}$ titration of full-length cardiac TnC.[35]

**Paramagnetic Relaxation Enhancement of cTnC in the States with and without $Ca^{2+}$.** Incorporation of a paramagnetic species into a protein results in distance-


dx.doi.org/10.1021/bi4000172 | Biochemistry 2013, 52, 1950−1962

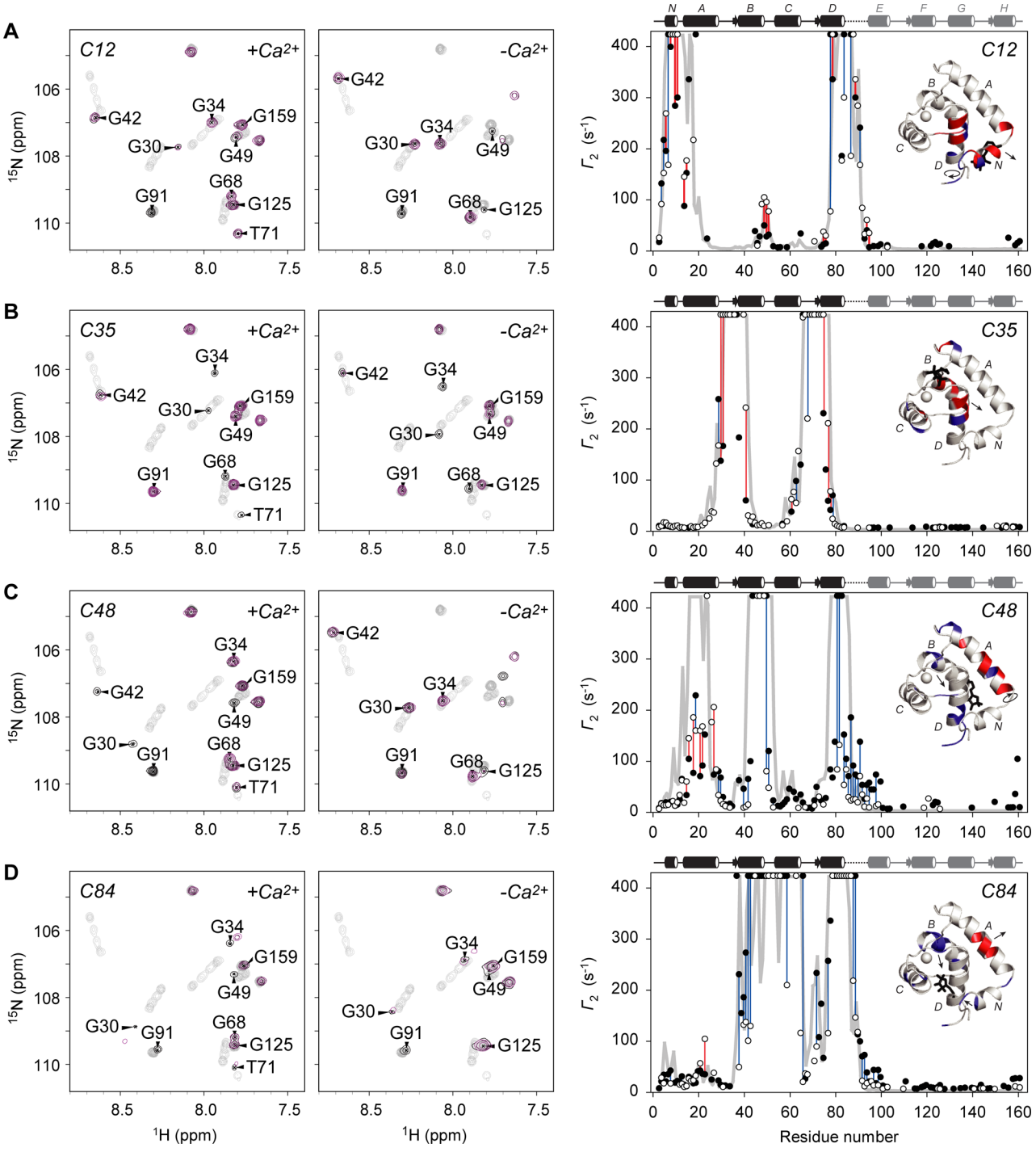


**Figure 3.** Representative section of the paramagnetic (maroon) and diamagnetic (black) $^{15}$N HSQC NMR spectra acquired for each spin-labeled cTnC construct in the presence (left) and absence (right) of $Ca^{2+}$: (A) C12, (B) C35, (C) C48, and (D) C84. The $Ca^{2+}$ titration series used for assignment of the spectra of the state without $Ca^{2+}$ are also shown (gray). Experimental PRE profiles ($\Gamma_2$) for each cTnC spin-labeled construct (far right) are shown in the states with $Ca^{2+}$ (●) and without $Ca^{2+}$ (○). For comparison, $\Gamma_2$ values back-calculated from the coordinates of the cTnC PDB structure (1AJ4[9]) are shown as solid gray lines. $\Gamma_2$ values of residues that could be measured in the states with and without $Ca^{2+}$ are mapped onto TnC (inset) and highlighted by connection with a blue line in cases where $\Gamma_2$ (with $Ca^{2+}$) > $\Gamma_2$ (without $Ca^{2+}$) or a red line in cases where $\Gamma_2$ (with $Ca^{2+}$) < $\Gamma_2$ (without $Ca^{2+}$).

dependent relaxation rate enhancement effects on nearby nuclei. In the case of nitroxide radicals, these effects are most accurately measured within the range of 10−25 Å. Therefore, to probe the conformation of the N-domain of cTnC, we made four monocysteine constructs (C12, C35, C48, and C84) and labeled each of these mutants with the stable nitroxide spin-label MTSL. The mutants were chosen so that, together, the PRE-derived distances from these four sites would allow for extensive overlapping coverage of the entire regulatory N-domain (Figure 1B). $^{15}$N HSQC spectra were acquired for each construct before and after spin labeling with MTSL. No large-scale perturbations were detected because of the introduction


dx.doi.org/10.1021/bi4000172 | Biochemistry 2013, 52, 1950−1962

of cysteine residues at any of the four sites or from the spin labeling with MTSL, as judged by the observation that chemical shift perturbations were confined to the immediate vicinity of the probe site, as we have previously reported for C84 and C35 constructs.[23]

$^{15}$N HSQC spectra were recorded for each of the four spin-labeled cTnC NMR samples both before and after reduction of the nitroxide group to its diamagnetic equivalent by the addition of ascorbic acid. For each labeled cTnC construct, both experiments were performed in the presence and absence of $Ca^{2+}$. A section of the paramagnetic and diamagnetic spectra acquired for each construct is shown in Figure 3. Peak assignments for each mutant were transferred from our previously assigned cTnC* $^{15}$N HSQC spectrum[23] to each $^{15}$N HSQC spectrum acquired in the state with $Ca^{2+}$. Small perturbations in chemical shifts were typically observed for resonances adjacent to the spin-labeled residue, leading to a small number of uncertain assignments for each construct in the state with $Ca^{2+}$. However, in all cases, at least 85% of the N-domain resonances were assignable.

Because the N-domain of TnC is $Ca^{2+}$ specific and C-domain sites III and IV are capable of binding $Ca^{2+}$ or $Mg^{2+}$, in our $Ca^{2+}$-free samples, 3 mM $MgCl_2$ was included in the NMR buffer to ensure that both the C-domain $Ca^{2+}$ and $Mg^{2+}$ sites were occupied and thus in a physiologically relevant ($Mg^{2+}$-bound) state. Under these conditions, $Mg^{2+}$ does not bind to $Ca^{2+}$ specific N-domain site II, and thus, an apo state is achieved. All references to the "apo" state from hereafter refer to that state of the N-domain only, because the C-domain is in a $Ca^{2+}/Mg^{2+}$-bound state in all experiments. The exchange of $Ca^{2+}$ for $Mg^{2+}$ in the C-domain was not found to cause any significant chemical shift changes; that is, it was equivalent to the initial titration point shown in Figure 2A. Again, peak positions in the spectra of the spin-labeled samples without $Ca^{2+}$ were assigned by tracing peak movement from the end point of the titration. Because the $Ca^{2+}$-induced chemical shift changes observed for each of the four spin-labeled constructs were found to be very similar to those observed for cTnC* (Figure S2 of the Supporting Information), this strategy allowed the assignment of most resonances in the state without $Ca^{2+}$, provided the peaks were first assigned in the state with $Ca^{2+}$.

The unpaired electron of the nitroxide group induces line broadening effects on nearby resonances in a distance-dependent manner. Dramatic line broadening effects were clearly observed for residues in the immediate vicinity and surroundings of the spin-labeled residue for each of the four sites used (Figure 3, left panels). The relaxation enhancement ($\Gamma_2$) caused by the spin-label was therefore calculated from the peak intensity ratios for all resonances that could be detected in both the paramagnetic and diamagnetic spectra (Figure S3 of the Supporting Information). For resonances close to the spin-label (<10 Å), the strong PRE broadened peaks beyond detection in the paramagnetic spectrum, and thus, $\Gamma_2$ could not be calculated. At distances greater than 25 Å, the peak intensity changes are typically too small to reliably quantify ($I_{para}/I_{dia} > 0.95$). For each construct, there were a small number of residues for which no peak intensity ratio could be reliably calculated, either because of peak overlap in crowded spectral regions or because of peak assignment uncertainty.

**N-Domain Movement upon $Ca^{2+}$ Binding Detected by PRE Effects.** For the purpose of examining the conformation of the N-domain and its response to $Ca^{2+}$, only PRE distances measured within the regulatory N-domain (intradomain measurements) were used. It is worth noting, however, that despite the upper limit of 25 Å, a number of interdomain PRE effects were present. We have previously shown that significant interdomain dynamics occurs within cTnC because of the flexibility of the central domain linker, thereby requiring an ensemble fitting approach to account for the interdomain PRE effects as a result of the dynamics of the system.[23] The interdomain PREs observed were not found to differ significantly between the states with and without $Ca^{2+}$, as seen in Figure 3, suggesting that the preferred ensemble of interdomain orientations sampled by the two globular domains does not differ significantly between the holo and apo states.

In contrast to the interdomain measurements, significant changes in PRE rates within the N-domain were detected upon comparison of the apo and holo states. These changes in PRE rates are mapped onto cTnC for each of the four constructs (Figure 3, right panels, insets), where a decrease in the PRE rate for a residue upon $Ca^{2+}$ binding (red) implies movement away from the spin-label to a longer distance in the holo state, whereas $Ca^{2+}$-induced increases in PRE rates (blue) suggest movement closer to the spin-label. Each of the four N-domain spin-labeled constructs, as a result of their variable positioning and orientation, provides a unique viewpoint for detecting $Ca^{2+}$-induced conformational changes; thus, a small degree of difference in the pattern of PRE changes is observed for each of the four labeled constructs.

For the C12-labeled construct, $Ca^{2+}$ binding led to a reduction in PREs for resonances located in helix N and at the N-terminal end of helix A, suggesting a movement of these regions away from the C12 spin-label upon $Ca^{2+}$ binding. Changes were also observed for helix D, where an alternating pattern of increased and decreased PREs most likely correlates to a counterclockwise rotation of helix D relative to the C12 spin-label position. Changes in PRE effects for helix D upon $Ca^{2+}$ binding were also observed from the C35 probe position, where the decreased PRE rates at the N-terminal end and increased PRE rates at the C-terminal end are suggestive of a tilting motion of helix D as indicated in Figure 3. Movement of helix B away from the C35 label upon $Ca^{2+}$ binding was also detected. From the C35 position, the differences were also observed for residues in helix A adjacent to the defunct $Ca^{2+}$ site I. Such changes are consistent with the $Ca^{2+}$-induced extension of this helix that is reported to occur in isolated TnC upon $Ca^{2+}$ binding.[6,12] The possible extension of helix A was also detected from the C48 probe site where $Ca^{2+}$ binding induced an alternating surface profile pattern for this helix that extended toward the N-terminus of the helix. This pattern suggests that a clockwise rotation of helix A may accompany the helix extension.

For the C84 spin-label, $Ca^{2+}$ binding increased PRE rates measured to residues of helix B, adjacent to $Ca^{2+}$ site I. Similar changes for residues in helix B were also revealed by the spin-label at C48. The effects observed for this helix are an interesting observation because the extension of helix B is described as the critical step for the transition to the open conformation that was observed in the presence of the TnI switch peptide or the cardiotonic drug bepridil.[6] Decreased PRE rates were also observed for residues located in the middle of helix A, which could be attributed to a bending of helix A, although this bending is not seen from any other spin-label viewpoint.


dx.doi.org/10.1021/bi4000172 | Biochemistry 2013, 52, 1950−1962

Table 1. Q Factor Values for Fits of Intradomain Cardiac TnC PRE Data

| | | with $Ca^{2+}$ | | without $Ca^{2+}$ | |
|---|---|---|---|---|---|
| PDB entry | | mean Q (standard deviation) | minimal Q (model[a]) | mean Q (standard deviation) | minimal Q (model[a]) |
| 1SPY | apo N-cTnC | 0.138 (0.006) | 0.129 (37) | 0.135 (0.005) | 0.124 (31) |
| 1AP4 | $Ca^{2+}$-N-cTnC | 0.124 (0.005) | 0.110 (38) | 0.127 (0.004) | 0.117 (34) |
| 1MXL | $Ca^{2+}$-N-cTnC-$TnI_{switch}$ | 0.150 (0.010) | 0.131 (22) | 0.148 (0.006) | 0.136 (23) |

[a]The model number of these "best fitting" structures (in parentheses in the minimal Q columns) corresponds to that listed in each of the PDB coordinate files.

Many of these PRE changes upon $Ca^{2+}$ binding, as mapped in Figure 3, show features consistent with a transition from the closed state to the primed state or the open state.[6,12,36] However, a final global assessment of the structural end point is difficult when local effects from each probe site are considered separately. This is because changes to the spin-label position itself upon $Ca^{2+}$ binding may result in the observed changes in the PRE rate. To assess the topology of a small globular domain, such as the five-helix N-cTnC of interest in this study, constraints derived from at least two probe sites are required to negate problems associated with changes in the spin-label position.[37] We therefore combined the PRE data from all four labeled constructs so we could best evaluate the global conformation of N-cTnC in each of its apo and holo states. This gave us a total of 208 distance measurements within the regulatory N-domain of TnC for the state with $Ca^{2+}$ and 183 measurements for the state without $Ca^{2+}$ (Figure S4 of the Supporting Information). Near complete coverage of the N-domain was attained with at least one distance constraint measured for 82 of a total of 89 N-domain residues in the state with $Ca^{2+}$ and a similar number observed for the $Ca^{2+}$-free state (80 of 89 residues) (Figure S4 of the Supporting Information). At least two constraints were obtained for the majority of N-domain residues, and constraints from each of the four spin-label sites for a small number of residues could also be measured.

The N-domain PRE measurements combined for all four spin-labeled constructs in the states with and without $Ca^{2+}$ were compared to three available solution structures of cardiac TnC determined under various experimental conditions: (i) apo N-cTnC (PDB entry 1SPY),[12] (ii) $Ca^{2+}$-N-cTnC (PDB entry 1AP4),[12] and (iii) $Ca^{2+}$-N-cTnC TnI switch peptide-bound state (PDB entry 1MXL).[5] Together, these structures have been described in the literature to essentially represent three different functional states of the regulatory domain of cTnC (Figure 1a). The metal-free structural model 1SPY represents a closed conformation state for the N-domain. The $Ca^{2+}$-bound structural model 1AP4, although described as essentially representing a closed conformation,[9,12] is best viewed as an activated or primed state.[6] Lastly, 1MXL represents an open conformation, stabilized by the presence of $Ca^{2+}$ and the bound TnI switch peptide.[5] Each of the three PDB structures utilized in this study comprises 40 models, with the variability within each family of structures being much smaller than the variation between each family.

To determine if a predominant conformation for the N-domain in both the calcium-bound and -free states could be identified using one of the three selected PDB sets, comparisons were made between our PRE measurements and each of the 40 models within the selected PDB ensembles, using the Q factor statistic (eq 3). The Q factors calculated for each structure within the PDB ensembles are shown in Figure S5 of the Supporting Information and are summarized in Table 1. The Q factor reports the ability of each model to account for the observed PRE effects where a smaller Q factor value indicates better agreement between the model and data.[38] The minimal Q factor value within each family of structures is also reported (Table 1).

The relatively low Q factor values obtained from the comparison of each of the three structural models to the combined PRE data sets from the four spin-labeled sites suggest that all three structures represent good models for the N-domain under both $Ca^{2+}$-bound and -free conditions. For both $Ca^{2+}$-bound and $Ca^{2+}$-free states, the same structural model (1AP4) gave the best fit to the experimental data, with the lowest Q factor obtained for the state with $Ca^{2+}$ (0.124). This analysis suggested that 1AP4 is the best structural representation of the predominant state of the N-domain, irrespective of the metal-bound state, under both apo and holo conditions. Higher Q factors were noted for 1MXL (0.148 and 0.150 for apo and holo, respectively), which is somewhat not unexpected, because the TnI switch peptide is required to stabilize the open conformation. It is important to note that, while higher Q factors were obtained for both 1MXL and 1SPY, the Q factor values allow us to infer only that neither structure is likely to represent the predominant state of N-cTnC. We cannot rule out the possibility of the existence of either structure as a minor species from this single-model analysis, as others have suggested may be the case.[8]

**Calcium Binding Changes the Open−Closed Equilibrium of N-cTnC.** The fact that the primed structure of 1AP4 best represents both the calcium-bound and -free states raises the possibility that there is little structural change upon $Ca^{2+}$ binding. However, this is unlikely to be the case as significant differences in PRE rates were measured for each of the four labeled constructs upon $Ca^{2+}$ binding, as shown in Figure 3, many of which appear to be consistent with a transition toward the open state observed in the presence of TnI.[5,6] For isolated TnC, any structural transition between the closed and open state is likely to occur in the fast exchange regime (nanoseconds to microseconds) on the chemical shift time scale.[8,15−17,36,39,40] We therefore sought to determine if the $Ca^{2+}$-induced differences we observed in the PRE rates were due to an alteration in the equilibrium between the closed form state (best represented by 1AP4) and the open conformation (represented by structural model 1MXL).

For such systems in fast exchange, the PRE rates represent the population ($p$)-weighted average of the PRE contributions arising from all conformational states.[41] Thus, if a significant proportion of the open conformation does exist in isolated TnC, then its imprint should be detectable in our measurements (eq 4).[42]

$$\Gamma_2^{obs} = p\Gamma_2^{open} + (1 - p)\Gamma_2^{closed} \quad (4)$$


dx.doi.org/10.1021/bi4000172 | Biochemistry 2013, 52, 1950−1962

The single Q factor values listed in Table 1 indicate that the primed 1AP4 structure was the best representative of the major species under both holo and apo conditions (Q = 0.124 and 0.127, respectively), from the three published TnC structures examined. Therefore, using the best fitting single conformer of 1AP4 to represent the closed/primed conformation and the best fitting single conformer of 1MXL to represent the open conformation, PREs were back-calculated for open and closed conformational states according to eq 2. A two-state equilibrium was then simulated using eq 4, where the population of the open conformation was increased from 0 to 1 in 0.01 increment steps to determine the fractions of the open ($p$) and closed conformational states ($1 - p$) that minimized the discrepancy between the observed and simulated PRE rates (as measured by Q factor analysis) (Figure 4).

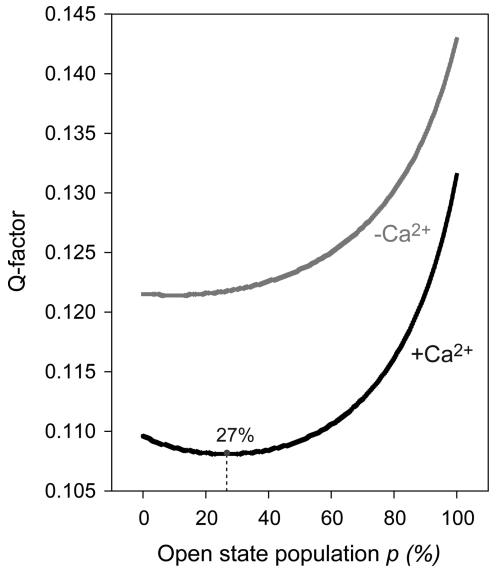


**Figure 4.** Q factors obtained from fitting a two-state model to the intradomain PREs. The ratio of the population of the open conformation (1MXL) compared to the closed conformation (1AP4) was increased from 0 to 1.0, in 0.01 increments. Q factors were calculated for states with (black) and without (gray) $Ca^{2+}$. PREs and the fraction of open conformer at which the lowest Q actor was obtained are also indicated.

For the experimental data set for the state without $Ca^{2+}$, no improvement in the Q factor was attained through the inclusion of small populations of the open state, with the Q factor remaining essentially the same for open state populations ranging from 0 to 15%. For an open state population with weightings above 15%, the Q factor clearly increased proportionally. Therefore, if an open conformation does exist in $Ca^{2+}$-free N-cTnC, its population must be less than 15%.

For the experimental data set for the state with $Ca^{2+}$, Q factor analysis using this two-state model led to a clear improvement in the fit to our PRE data when a small fraction of the open conformation was included. The open state population that yielded the lowest Q factors was identified at ~27%, suggesting that the holo state of cTnC samples a more open conformation than the apo state for a significant proportion of time.

**Structural Consequences of the A8V FHC Mutation.** The A8V hypertrophic cardiomyopathy mutation located in helix N of cardiac TnC was recently shown to alter $Ca^{2+}$ affinity and affect force recovery in skinned muscle fibers.[19] A mechanism through which this mutation affects TnC function is not, however, established. Previous modeling of circular dichroism data for the A8V mutation in isolated TnC suggested this mutation may lead to changes in the secondary structure content for both the apo and holo states.[43] Therefore, to assess the structural consequences arising from the A8V mutation in isolated TnC, we measured PREs for the C84 protein into which the FHC A8V mutation had been introduced (Figure 5A).

The overall appearances of the $^{15}N$ HSQC spectra acquired for holo A8V and holo TnC (C84) in the $Ca^{2+}$-loaded state were found to be quite similar (Figure S6A,B of the Supporting Information), with good dispersal and narrow line widths. The assignments of the native TnC construct were transferred to the A8V spectrum, and chemical shift perturbations were analyzed (Figure 5B). In the $Ca^{2+}$-bound state, the A8V mutation caused large chemical shift perturbations for adjacent residues located in helix N. Significant perturbations ($\delta_{av} > 0.1$) were also observed within the defunct $Ca^{2+}$ metal binding site I and also helix D.

In the $Ca^{2+}$-free state, notable differences between the A8V and native constructs were apparent in the spectra (Figure S6C,D of the Supporting Information). Despite the presence of $Mg^{2+}$, the spectrum of A8V showed signs of disorder for both C-domain metal sites III and IV, similar to that observed within cTnC* in the metal-free state (Figure S1A of the Supporting Information). This disorder was not observed in the native construct acquired under the same $Ca^{2+}$-free conditions (Figure S6D of the Supporting Information). While the assignment of many C-domain peaks of A8V in the $Ca^{2+}$-free $^{15}N$ HSQC spectrum was not possible, the assignments of the N-domain peaks of the native construct in the $Ca^{2+}$-free state were able to be transferred to the A8V mutant in most cases. In the $Ca^{2+}$-free state, the A8V mutation was found to induce significant chemical shift changes throughout the entire N-domain (Figure 5B); large perturbations ($\delta_{av} > 0.1$) were observed within all structural elements of the N-domain, with the largest perturbations arising from residues located in the N-helix, the defunct $Ca^{2+}$ site I, and the functional $Ca^{2+}$ site II. On the basis of the chemical shift data and the appearance of the HSQC spectra, it appears that the structural perturbation of the A8V mutation is more severe in the apo state, encompassing the entire cTnC molecule.

The PRE rates measured from the C84 spin-label in the absence and presence of the A8V mutation in the apo and holo states are shown in panels C and D of Figure 5, respectively. Residues that could be assigned in both constructs are highlighted, and the directional change in PRE rates due to the presence of the FHC mutation is also indicated, both on the PRE profile and on the structure. In the holo state, the differences in PRE rates observed for helices N and A for the A8V mutant construct indicate either a change in the N–A interhelical angle or disruption of helix N and subsequent unwinding of this region, although the latter appears unlikely as the N and HN chemical shifts were not found to shift toward random coil values.[44] Effects caused by the A8V mutation were also apparent in the vicinity of the defunct $Ca^{2+}$ site I that moved toward the C84 spin-label, although an alteration in the dynamics of this region may also account for the PRE rate differences observed. The reduced PRE rates of helix B residues indicated movement away from the C84 spin-label, whereas no notable differences were detected for residues in helix C. Of note is the fact that these regions that were found to differ


dx.doi.org/10.1021/bi4000172 | Biochemistry 2013, 52, 1950−1962

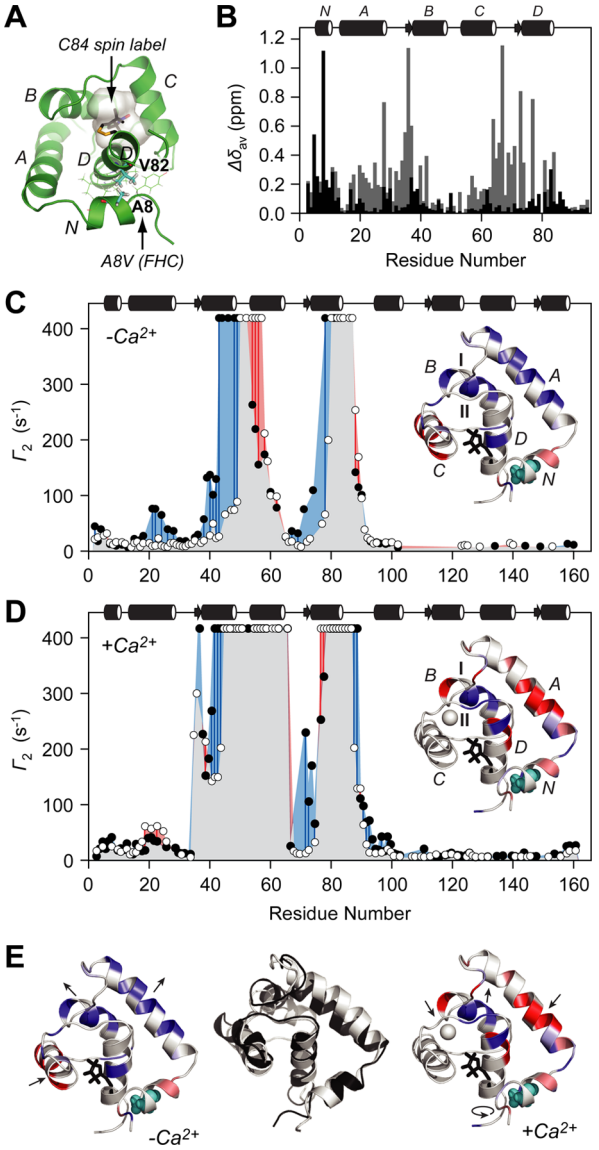


**Figure 5.** Location of the A8V familial hypertrophic cardiomyopathy mutation in the N-domain of TnC[19] and spin-label site C84. (B) Chemical shift differences ($\Delta\delta_{av}$) between native and A8V cTnC spin-labeled constructs for each residue that can be assigned in the diamagnetic HSQC spectra, derived from $^{1}H$ and $^{15}N$ chemical shifts in the states without (gray) and with (black) $Ca^{2+}$. (C and D) Comparison of the PRE rates ($\Gamma_2$) measured for the A8V mutant (○) and native cTnC (●) in the states without (C) and with (D) $Ca^{2+}$. Paired measurements are highlighted by connection with a blue line in cases where $\Gamma_2$[WT] > $\Gamma_2$[A8V] or a red line in cases where $\Gamma_2$[WT] < $\Gamma_2$[A8V]. The differences in $\Gamma_2$ are mapped onto N-cTnC (PDB entry 1AP4[12]) using the same coloring, and helices N and A–D, along with sites I and II, are indicated. (E) Direction of movement suggested by the changes in PRE rates obtained in the $Ca^{2+}$-free (left) and $Ca^{2+}$-bound (far right) states indicated with arrows. For comparison of the mapped PRE differences obtained in the presence of the A8V mutation, the closed (gray) and open (black) N-domain structures previously observed in cTnC[5,12] are shown aligned at the C84 spin-label position on helix D (middle panel). The differences seen in the state with $Ca^{2+}$ are consistent with movement toward the open structure. In the state without $Ca^{2+}$, movement appears to be toward a unique open state not previously seen in cTnC.

between native and A8V proteins in the holo state align remarkably well with the movement expected for a closed to open conformational change (Figure 5E). Together, the changes observed suggest that, in the holo state, the net effect of the A8V mutation is to move the N-domain toward a more open conformation, similar to that observed in the presence of TnI, thus likely modifying the interaction with the $TnI_{switch}$ region.

Significant structural perturbations within the N-domain were also detected in the $Ca^{2+}$-free state. The A8V mutation decreased the PRE rates for resonances located in helices A and B, suggesting that these elements are located farther from the central C84 spin-label. Helix C moved closer to the labeled sites as indicated by the increased PRE rates. Other small differences were also observed for residues at the N–D interface, at the site of the FHC mutation. Taken together, in the apo state the A8V mutation appears result in a conformation more open than that observed in the native protein. This open form is not comparable to the open state observed in the presence of TnI, as shown in Figure 5E, but rather is a unique open conformation not previously observed for cTnC.

## DISCUSSION

The cardiac isoform of TnC is widely discussed as a potential target for the development of inotropic model compounds, better known as "calcium-sensitizer" drugs, for the treatment of congestive heart failure and other cardiac disorders.[45] Drugs such as bepridil, trifluoperazine, anapoe, and levosimendan appear to function by altering the open–closed equilibrium of TnC.[45] However, despite the availability of several high-resolution structures depicting an open conformation of the N-domain of cardiac TnC bound with the switch region of TnI,[4,5] a clear description of the dynamic exchange between the closed and open events triggered by $Ca^{2+}$ binding, which is important for rational drug design and development, does not exist. Although several studies have suggested that both open and closed structural states exist for the $Ca^{2+}$-saturated cardiac TnC isoform,[8,15,16] a true open state has not been observed experimentally for the $Ca^{2+}$-saturated state in isolation. In contrast, the binding of $Ca^{2+}$ to the regulatory N-domain of the skeletal isoform triggers a distinct conformational change to expose a hydrophobic patch within the N-domain to which $TnI_{switch}$ subsequently binds.[13]

Our results using the technique of PRE-NMR in cardiac TnC in the presence of calcium have detected a population of ~27% of the N-domain of TnC that exists in the open conformation that is observed when the switch peptide of TnI is bound. In the absence of $Ca^{2+}$, the population of the open state, if present at all, is significantly smaller (~15% at most). Thus, binding of $Ca^{2+}$ to the cardiac isoform creates a dynamic equilibrium between closed and open conformational states, shifting the population to the open state, thereby priming the regulatory domain of cTnC to bind with TnI via conformational selection. That is, the switch peptide region of TnI is not essential for triggering the opening of the N-domain as both the closed and open conformations are detected simultaneously in isolated TnC.

**The Apo N-Domain of cTnC Is in a Primed State.** We initially compared our PRE measurements from the four unique spin-labeled sites to the high-resolution NMR structures representing three recognized functional states of TnC, namely, an apo state (1SPY[12]), a $Ca^{2+}$-loaded state (1AP4[12]), and the $Ca^{2+}$-loaded bound switch peptide state (1MXL[5]). This comparison suggested that the $Ca^{2+}$-loaded conformation of 1AP4 is the best representation of the N-domain in the holo


dx.doi.org/10.1021/bi4000172 | Biochemistry 2013, 52, 1950–1962

state. Our results indicated that the same $Ca^{2+}$-loaded NMR structure (1AP4) was also the best representation for the PRE-NMR constraints obtained in the absence of $Ca^{2+}$ and not the NMR structure of $Ca^{2+}$-free N-TnC (1SPY). While the structures for the holo and apo N-domain of isolated TnC (1AP4 and 1SPY, respectively) are described in the literature to essentially represent closed conformations of the N-domain,[12] there are small differences between these two structures. The most prominent differences are the extensions of helices A and C and the subsequent 10° alteration of the C−D interhelical angle triggered by binding of $Ca^{2+}$ to sites I and II.[6,12] While this 10° change is much smaller than the 40° change in the C−D interhelical angle that is required for the transition to the open conformation observed in the presence of $TnI_{switch}$, as seen in 1MXL,[5] it does constitute a small opening transition from a compact closed state (as in 1SPY) to a less compact but still closed conformational state (as in 1AP4).[12] Because the PRE method is biased toward distances of closest approach due to the strong distance dependence of the PRE effect ($\Gamma_2 \propto r^{-6}$),[41,46] it is intrinsically more sensitive to the shorter distances that are found in compact states. The observation that the fits to our PRE data selected for the lesser of the two compact closed structures therefore also strongly supports the result that 1SPY is unlikely to represent the predominant conformation of the apo state of the N-domain. While it is possible that our spin-labels have induced a structural state under apo conditions different from that presented by 1SPY, we believe that this is unlikely, because there was minimal global structural perturbation of the N-domain from our four spin-label sites, as judged by chemical shift analysis. Rather, our analysis suggests that structures obtained under the same physiological conditions for the isolated N-TnC domain differ from the structures of N-TnC obtained in full-length TnC.

**$Ca^{2+}$ Binding Increases the Population of the Open State.** Data presented here best support a dynamic equilibrium model for describing the conformational events that the regulatory domain of cTnC undergoes during muscle contraction. That is, the regulatory domain of isolated cTnC in solution largely exists in equilibrium between closed and open states, with the closed state best represented by the 1AP4 structure. This equilibrium was first proposed by Pääkkönen et al.,[8] who observed exchange broadening for residues located in the hinge regions involved in the domain opening transition in the presence of $Ca^{2+}$. As the equilibrium between the closed and open conformational states is in the fast exchange regime,[8,40] the proportion of conformers adopting the closed versus open conformation can be quantified from the measured PRE rate, for both the apo and holo data sets.[47] By fitting our PRE measurements to a two-state model of the open−closed equilibrium of N-cTnC and identifying the open state population at which the Q factor is minimized, we have indeed found that $Ca^{2+}$ binding does increase the population of the open state. Our results show that if the open state is present in the $Ca^{2+}$-free state, its population must be <15%. When $Ca^{2+}$ binds, the open state population increases to ∼27%. Our observations are also in agreement with recent molecular dynamics studies that showed that the open conformation is present for $Ca^{2+}$-saturated cTnC in the absence of TnI[36,40] and close to the prediction, made on the basis of free energy calculations, of 16% of $Ca^{2+}$-loaded N-cTnC being present in an open conformation in the absence of TnI.[18] Although an open population of only 27% may appear to be low for full activation of muscle, our findings do suggest that any modification of the N-domain of cTnC, whether from a disease mutation or binding of an inotropic compound, is likely to lead to the disruption of the structural and dynamic properties of the N-domain, leading to impaired function.

While the experiments presented here were performed on isolated TnC, the biological implications of these findings are apparent for the troponin complex. Li et al.[5] demonstrated that $Ca^{2+}$ is required for the switch peptide to bind to TnC and, more importantly, the regulatory N-domain has to be an open state for the TnI switch peptide to bind. Other studies in the presence of TnI and $Ca^{2+}$ on the cardiac isoform by Gaponeko et al. show that in addition to the population of the open state increasing, conformational exchange between the open and closed states still occurs. It then follows from our observation that an increased population of the open state as a result of $Ca^{2+}$ binding would then increase the probability of the TnI switch peptide colliding with N-TnC in a binding-competent (open) conformation. Demonstrating how alterations in cTnC dynamics triggered simply by $Ca^{2+}$ binding effectively propagate through the troponin complex is still experimentally challenging. However, what seems apparent from our study and others is that dynamics plays a key role in fine-tuning the $Ca^{2+}$ troponin switch regulatory mechanism for the cardiac isoform. The phosphorylation state of the unique cardiac TnI N-extension is also suggested to alter the equilibrium between the open and closed states[15] and will be the subject of future studies using this NMR approach.

**The A8V Mutation Opens the Regulatory N-Domain of cTnC.** Several detrimental hypertrophic cardiomyopathy (HCM) and dilated cardiomyopathy (DCM) mutations are found clustered in the proximity of each of the metal-binding regions of the cardiac isoform of TnC, including the defunct site I.[48] Therefore, shedding light on the structural nature of $Ca^{2+}$ signaling is also important for understanding these diseases that are associated with impaired $Ca^{2+}$ handling. A primary motivation for this study was to also assess the suitability of the PRE-NMR approach for rapidly examining structural perturbations resulting from disease-causing mutations. Using our spin labeling strategy to characterize the hypertrophic cardiomyopathy-linked A8V mutation,[49] we have established that the PRE approach, in combination with measurements of chemical shift changes, can be utilized as a rapid screening tool to assess structural perturbations arising from such disease-causing mutations. While chemical shift perturbation analysis alone is capable of highlighting regions that may differ structurally, PRE is capable of indicating the direction of change. However, care with the targeted placement of the spin-label reporter group is required to be sufficiently sensitive to detect potential changes in the helical packing of the N-domain arising from a disease-causing mutation. The most appropriate position for capturing changes upon $Ca^{2+}$ binding was by positioning the label in the center of the N-domain on helix D (C84) (Figure 5A).

The PRE data showed that incorporation of the A8V mutation resulted in significant structural perturbation in both the apo and holo states of c-TnC. Our results also supported the first report of structural perturbation arising from this mutation, obtained in the circular dichroism investigation of Pinto et al.[43] In the holo state, the changes in PRE rates caused by the A8V mutation were consistent with an opening of the regulatory domain, similar to that observed in the presence of TnI. In the apo state, the perturbations to cTnC were more severe, affecting all helices within the N-domain. The outward


dx.doi.org/10.1021/bi4000172 | Biochemistry 2013, 52, 1950−1962

movement of helices revealed by the PRE data suggested movement toward an alternative open conformation, not previously observed in cTnC. While our rapid single-probe screening strategy with the label at residue 84 effectively demonstrated a perturbation of the TnC subunit and allowed for a description of the major structural effects arising from a disease-causing mutation (A8V), it is important to note that it cannot definitively describe the atomic structure resulting from the mutation. Whether the changes seen in each state are due to a change in the predominant conformation of the N-domain or rather an alteration to the population of the open conformation would require the placement of probes at additional sites.[37]

Although the regulatory N-domain of cTnC was the focus of this study, it is interesting to note that our spectra suggested that the A8V mutation also altered the metal binding affinity of sites III and IV in the C-domain. While this finding may seem surprising given that the N- and C-domains are thought to be structurally independent, similar interdomain metal binding affinity perturbations arising from mutations in helix N of the N-domain have previously been reported. For example, the deletion of residues 1−14 of helix N was reported to alter binding of $Ca^{2+}$ to sites III and IV.[50] While the mechanism through which such interdomain effects occur is unclear, an interaction between helix N and the central linker has been suggested to occur in cTnC.[51] We have also previously shown that cTnC preferentially adopts compact interdomain orientations such that interdomain contacts between the N- and C-domains are likely.[23] With the results presented here and in light of the recent report of another cTnC helix N mutant (Y5H) being linked to DCM,[52] it appears that helix N of cTnC does indeed have some, as of yet, unidentified functional role in the cardiac regulatory mechanism. It is possible that only through the inclusion of the other two troponin subunits may its role be fully elucidated, and thus, further investigation is warranted.

## ■ ASSOCIATED CONTENT

### Supporting Information

$^{15}N$ HSQC NMR spectra acquired during the $Ca^{2+}$ titration of the C-domain of cTnC (Figure S1), chemical shift changes that caused binding of $Ca^{2+}$ to the N-domain of cTnC constructs (Figure S2), peak intensity ratios measured for each cTnC construct in the state with $Ca^{2+}$ (Figure S3), visual display of the coverage of the N-domain obtained from our four spin-label positions (Figure S4), the distribution of $Q$ factors for all PDB ensembles (Figure S5), and comparison of paramagnetic and diamagnetic $^{15}N$ HSQC spectra acquired for native cTnC and cTnC A8V in the $Ca^{2+}$-free and $Ca^{2+}$-bound states (Figure S6). This material is available free of charge via the Internet at http://pubs.acs.org.

## ■ AUTHOR INFORMATION


### Corresponding Author

*E-mail: louise.brown@mq.edu.au. Telephone: +61 2 9850 8294. Fax: +61 2 9850 8313.

### Present Addresses

[‖]Molecular Cardiology and Biophysics Division, Victor Chang Cardiac Research Institute, 405 Liverpool St., Darlinghurst, NSW 2010, Australia.

[⊥]Menzies Research Institute, University of Tasmania, TAS 7000, Australia.



### Funding

This work was funded by the National Health and Medical Research Council of Australia (Grant 434220) and a Macquarie University research development grant to L.J.B. N.M.C. was supported by an Australian Postgraduate Award.


### Notes

The authors declare no competing financial interest.

## ■ ACKNOWLEDGMENTS


We are grateful to Professor Paul Curmi, Professor Timothy Logan, and Dr. James Cooke for many helpful discussions.


## ■ ABBREVIATIONS

cTnC, cardiac troponin C; skTnC, skeletal troponin C; PRE, paramagnetic relaxation enhancement; cTnC*, cysteine-less cTnC construct; PDB, Protein Data Bank.

## ■ REFERENCES


(1) Gordon, A. M., Homsher, E., and Regnier, M. (2000) Regulation of contraction in striated muscle. *Physiol. Rev. 80*, 853−924.

(2) Li, M. X., Wang, X., and Sykes, B. D. (2004) Structural based insights into the role of troponin in cardiac muscle pathophysiology. *J. Muscle Res. Cell Motil. 25*, 559−579.

(3) Metzger, J. M., and Westfall, M. V. (2004) Covalent and noncovalent modification of thin filament action: The essential role of troponin in cardiac muscle regulation. *Circ. Res. 94*, 146−158.

(4) Takeda, S., Yamashita, A., Maeda, K., and Maeda, Y. (2003) Structure of the core domain of human cardiac troponin in the $Ca^{2+}$-saturated form. *Nature 424*, 35−41.

(5) Li, M. X., Spyracopoulos, L., and Sykes, B. D. (1999) Binding of cardiac troponin-I147−163 induces a structural opening in human cardiac troponin-C. *Biochemistry 38*, 8289−8298.

(6) Li, Y., Love, M. L., Putkey, J. A., and Cohen, C. (2000) Bepridil opens the regulatory N-terminal lobe of cardiac troponin C. *Proc. Natl. Acad. Sci. U.S.A. 97*, 5140−5145.

(7) McKay, R. T., Pearlstone, J. R., Corson, D. C., Gagne, S. M., Smillie, L. B., and Sykes, B. D. (1998) Structure and interaction site of the regulatory domain of troponin-C when complexed with the 96−148 region of troponin-I. *Biochemistry 37*, 12419−12430.

(8) Pääkkönen, K., Annila, A., Sorsa, T., Pollesello, P., Tilgmann, C., Kilpeläinen, I., Karisola, P., Ulmanen, I., and Drakenberg, T. (1998) Solution structure and main chain dynamics of the regulatory domain (residues 1−91) of human cardiac troponin C. *J. Biol. Chem. 273*, 15633−15638.

(9) Sia, S. K., Li, M. X., Spyracopoulos, L., Gagne, S. M., Liu, W., Putkey, J. A., and Sykes, B. D. (1997) Structure of cardiac muscle troponin C unexpectedly reveals a closed regulatory domain. *J. Biol. Chem. 272*, 18216−18221.

(10) Slupsky, C. M., and Sykes, B. D. (1995) NMR solution structure of calcium-saturated skeletal muscle troponin C. *Biochemistry 34*, 15953−15964.

(11) Spyracopoulos, L., Gagne, S. M., Li, M. X., and Sykes, B. D. (1998) Dynamics and thermodynamics of the regulatory domain of human cardiac troponin C in the apo- and calcium-saturated states. *Biochemistry 37*, 18032−18044.

(12) Spyracopoulos, L., Li, M. X., Sia, S. K., Gagne, S. M., Chandra, M., Solaro, R. J., and Sykes, B. D. (1997) Calcium-induced structural transition in the regulatory domain of human cardiac troponin C. *Biochemistry 36*, 12138−12146.

(13) Gagne, S. M., Tsuda, S., Li, M. X., Smillie, L. B., and Sykes, B. D. (1995) Structures of the troponin C regulatory domains in the apo and calcium-saturated states. *Nat. Struct. Mol. Biol. 2*, 784−789.

(14) Vinogradova, M. V., Stone, D. B., Malanina, G. G., Karatzaferi, C., Cooke, R., Mendelson, R. A., and Fletterick, R. J. (2005) $Ca^{2+}$-regulated structural changes in troponin. *Proc. Natl. Acad. Sci. U.S.A. 102*, 5038−5043.

(15) Gaponenko, V., Abusamhadneh, E., Abbott, M. B., Finley, N., Gasmi-Seabrook, G., Solaro, R. J., Rance, M., and Rosevear, P. R. (1999) Effects of troponin I phosphorylation on conformational exchange in the regulatory domain of cardiac troponin C. *J. Biol. Chem. 274*, 16681−16684.
(16) Pääkkönen, K., Sorsa, T., Drakenberg, T., Pollesello, P., Tilgmann, C., Permi, P., Heikkinen, S., Kilpeläinen, I., and Annila, A. (2000) Conformations of the regulatory domain of cardiac troponin C examined by residual dipolar couplings. *Eur. J. Biochem. 267*, 6665−6672.
(17) Dong, W.-J., Xing, J., Villain, M., Hellinger, M., Robinson, J. M., Chandra, M., Solaro, R. J., Umeda, P. K., and Cheung, H. C. (1999) Conformation of the regulatory domain of cardiac muscle troponin C in its complex with cardiac troponin I. *J. Biol. Chem. 274*, 31382−31390.
(18) Gagné, S. M., Li, M. X., McKay, R. T., and Sykes, B. D. (1998) The NMR angle on troponin C. *Biochem. Cell Biol. 76*, 302−312.
(19) Landstrom, A. P., Parvatiyar, M. S., Pinto, J. R., Marquardt, M. L., Bos, J. M., Tester, D. J., Ommen, S. R., Potter, J. D., and Ackerman, M. J. (2008) Molecular and functional characterization of novel hypertrophic cardiomyopathy susceptibility mutations in TNNC1-encoded troponin C. *J. Mol. Cell. Cardiol. 45*, 281−288.
(20) Brown, L. J., Sale, K. L., Hills, R., Rouviere, C., Song, L., Zhang, X., and Fajer, P. G. (2002) Structure of the inhibitory region of troponin by site directed spin labeling electron paramagnetic resonance. *Proc. Natl. Acad. Sci. U.S.A. 99*, 12765−12770.
(21) Dong, W.-j., Rosenfeld, S. S., Wang, C.-K., Gordon, A. M., and Cheung, H. C. (1996) Kinetic studies of calcium binding to the regulatory site of troponin C from cardiac muscle. *J. Biol. Chem. 271*, 688−694.
(22) Putkey, J. A., Dotson, D. G., and Mouawad, P. (1993) Formation of inter- and intramolecular disulfide bonds can activate cardiac troponin C. *J. Biol. Chem. 268*, 6827−6830.
(23) Cordina, N. M., Liew, C. K., Gell, D. A., Fajer, P. G., Mackay, J. P., and Brown, L. J. (2012) Interdomain orientation of cardiac troponin C characterized by paramagnetic relaxation enhancement NMR reveals a compact state. *Protein Sci. 21*, 1376−1387.
(24) Sambrook, J., Fritsch, E. F., and Maniatis, T. (1989) *Molecular cloning: A laboratory manual*, 2nd ed., Cold Spring Harbor Laboratory Press, Plainview, NY.
(25) Gay, G. L., Lindhout, D. A., and Sykes, B. D. (2004) Using lanthanide ions to align troponin complexes in solution: Order of lanthanide occupancy in cardiac troponin C. *Protein Sci. 13*, 640−651.
(26) Donaldson, L. W., Skrynnikov, N. R., Choy, W. Y., Muhandiram, D. R., Sarkar, B., Forman-Kay, J. D., and Kay, L. E. (2001) Structural characterization of proteins with an attached ATCUN motif by paramagnetic relaxation enhancement NMR spectroscopy. *J. Am. Chem. Soc. 123*, 9843−9847.
(27) Goddard, T. D., and Kneller, D. G. (2007) *SPARKY 3*, University of California, San Francisco.
(28) Volkov, A. N., Worrall, J. A. R., Holtzmann, E., and Ubbink, M. (2006) Solution structure and dynamics of the complex between cytochrome c and cytochrome c peroxidase determined by paramagnetic NMR. *Proc. Natl. Acad. Sci. U.S.A. 103*, 18945−18950.
(29) Battiste, J. L., and Wagner, G. (2000) Utilization of site-directed spin labeling and high-resolution heteronuclear nuclear magnetic resonance for global fold determination of large proteins with limited nuclear Overhauser effect data. *Biochemistry 39*, 5355−5365.
(30) Liang, B., Bushweller, J. H., and Tamm, L. K. (2006) Site-sirected parallel spin-labeling and paramagnetic relaxation enhancement in structure determination of membrane proteins by solution NMR spectroscopy. *J. Am. Chem. Soc. 128*, 4389−4397.
(31) Iwahara, J., Schwieters, C. D., and Clore, G. M. (2004) Ensemble approach for NMR structure refinement against $^{1}$H paramagnetic relaxation enhancement data arising from a flexible paramagnetic group attached to a macromolecule. *J. Am. Chem. Soc. 126*, 5879−5896.
(32) Spyracopoulos, L., Lavigne, P., Crump, M. P., Gagné, S. M., Kay, C. M., and Sykes, B. D. (2001) Temperature dependence of dynamics and thermodynamics of the regulatory domain of human cardiac troponin C. *Biochemistry 40*, 12541−12551.
(33) Cornilescu, G., Marquardt, J. L., Ottiger, M., and Bax, A. (1998) Validation of protein structure from anisotropic carbonyl chemical shifts in a dilute liquid crystalline phase. *J. Am. Chem. Soc. 120*, 6836−6837.
(34) Holroyde, M. J., Robertson, S. P., Johnson, J. D., Solaro, R. J., and Potter, J. D. (1980) The calcium and magnesium binding sites on cardiac troponin and their role in the regulation of myofibrillar adenosine triphosphatase. *J. Biol. Chem. 255*, 11688−11693.
(35) Li, M., Saude, E., Wang, X., Pearlstone, J., Smillie, L., and Sykes, B. (2002) Kinetic studies of calcium and cardiac troponin I peptide binding to human cardiac troponin C using NMR spectroscopy. *Eur. Biophys. J. 31*, 245−256.
(36) Lindert, S., Kekenes-Huskey, P. M., Huber, G., Pierce, L., and McCammon, J. A. (2012) Dynamics and calcium association to the N-terminal regulatory domain of human cardiac troponin C: A multiscale computational study. *J. Phys. Chem. B 116*, 8449−8459.
(37) Chen, H., Ji, F., Olman, V., Mobley, C. K., Liu, Y., Zhou, Y., Bushweller, J. H., Prestegard, J. H., and Xu, Y. (2011) Optimal mutation sites for PRE data collection and membrane protein structure prediction. *Structure 19*, 484−495.
(38) Cornilescu, G., Marquardt, J. L., Ottiger, M., and Bax, A. (1998) Validation of protein structure from anisotropic carbonyl chemical shifts in a dilute liquid crystalline phase. *J. Am. Chem. Soc. 120*, 6836−6837.
(39) Gagné, S. M., Sykes, M. T., and Sykes, B. D. (1998) The regulatory domain of troponin C: To be flexible or not to be flexible. *Journal of the Korean Magnetic Resonance Society 2*, 131−140.
(40) Lindert, S., Kekenes-Huskey, P. M., and McCammon, J. A. (2012) Long-timescale molecular dynamics simulations elucidate the dynamics and kinetics of exposure of the hydrophobic patch in troponin C. *Biophys. J. 103*, 1784−1789.
(41) Clore, G. M., and Iwahara, J. (2009) Theory, practice, and applications of paramagnetic relaxation enhancement for the characterization of transient low-population states of biological macromolecules and their complexes. *Chem. Rev. 109*, 4108−4139.
(42) Iwahara, J., and Clore, G. M. (2006) Detecting transient intermediates in macromolecular binding by paramagnetic NMR. *Nature 440*, 1227−1230.
(43) Pinto, J. R., Parvatiyar, M. S., Jones, M. A., Liang, J., Ackerman, M. J., and Potter, J. D. (2009) A Functional and structural study of troponin C mutations related to hypertrophic cardiomyopathy. *J. Biol. Chem. 284*, 19090−19100.
(44) Wang, Y., and Jardetzky, O. (2002) Probability-based protein secondary structure identification using combined NMR chemical-shift data. *Protein Sci. 11*, 852−861.
(45) Li, M. X., Robertson, I. M., and Sykes, B. D. (2008) Interaction of cardiac troponin with cardiotonic drugs: A structural perspective. *Biochem. Biophys. Res. Commun. 369*, 88−99.
(46) Tang, C., Schwieters, C. D., and Clore, G. M. (2007) Open-to-closed transition in apo maltose-binding protein observed by paramagnetic NMR. *Nature 449*, 1078−1082.
(47) Anthis, N. J., Doucleff, M., and Clore, G. M. (2011) Transient, sparsely populated compact states of apo and calcium-loaded calmodulin probed by paramagnetic relaxation enhancement: Interplay of conformational selection and induced fit. *J. Am. Chem. Soc. 133*, 18966−18974.
(48) Willott, R. H., Gomes, A. V., Chang, A. N., Parvatiyar, M. S., Pinto, J. R., and Potter, J. D. (2010) Mutations in troponin that cause HCM, DCM AND RCM: What can we learn about thin filament function? *J. Mol. Cell. Cardiol. 48*, 882−892.
(49) Rospigliosi, C. C., McClendon, S., Schmid, A. W., Ramlall, T. F., Barré, P., Lashuel, H. A., and Eliezer, D. (2009) E46K Parkinson's-linked mutation enhances C-terminal-to-N-terminal contacts in $\alpha$-synuclein. *J. Mol. Biol. 388*, 1022−1032.
(50) Smith, L., Greenfield, N. J., and Hitchcock-DeGregori, S. E. (1994) The effects of deletion of the amino-terminal helix on troponin C function and stability. *J. Biol. Chem. 269*, 9857−9863.

(51) Ding, X.-L., Akella, Á. B., Su, H., and Gulati, J. (1994) The role of glycine (residue 89) in the central helix of EF-hand protein troponin-C exposed following amino-terminal $\alpha$-helix deletion. *Protein Sci.* 3, 2089−2096.
(52) Hershberger, R. E., Norton, N., Morales, A., Li, D., Siegfried, J. D., and Gonzalez-Quintana, J. (2010) Coding sequence rare variants identified in MYBPC3, MYH6, TPM1, TNNC1, and TNNI3 from 312 patients with familial or idiopathic dilated cardiomyopathy. *Circ.: Cardiovasc. Genet.* 3, 155−161.
(53) Farmer, B. T., Constantine, K. L., Goldfarb, V., Friedrichs, M. S., Wittekind, M., Yanchunas, J., Robertson, J. G., and Mueller, L. (1996) Localizing the $NADP^+$ binding site on the MurB enzyme by NMR. *Nat. Struct. Mol. Biol.* 3, 995−997.